Universality of Block Copolymer Melts

Jens Glaser,[1,†] Pavani Medapuram,[1] Thomas M. Beardsley,[2] Mark W. Matsen,[2,‡] and David C. Morse[1,*]
[1]*Department of Chemical Engineering and Materials Science, University of Minnesota,*
421 Washington Avenue SE, Minneapolis, Minnesota 55455, USA
[2]*School of Mathematical and Physical Sciences, University of Reading,*
Whiteknights, Reading RG6 6AX, United Kingdom
(Received 4 February 2014; published 8 August 2014)

Simulations of five different coarse-grained models of symmetric diblock copolymers are compared to demonstrate a universal (i.e., model-independent) dependence of the free energy and order-disorder transition (ODT) on the invariant degree of polymerization $\bar{N}$. The actual values of χN at the ODT approach predictions of the Fredrickson-Helfand (FH) theory for $\bar{N} \gtrsim 10^4$ but significantly exceed FH predictions at lower values characteristic of most experiments. The FH theory fails for modest $\bar{N}$ because the competing phases become strongly segregated near the ODT, violating an underlying assumption of weak segregation.

DOI: 10.1103/PhysRevLett.113.068302 PACS numbers: 82.35.Jk, 64.60.De, 64.70.km

Universality is a powerful feature of polymer physics that allows the behavior of real systems to be predicted on the basis of simple generic models. The best example of this is the scaling theory of dilute and semidilute polymer solutions in good solvent [1–3]. This theory predicts a universal dependence on two thermodynamic state parameters—an excluded volume parameter and an overlap parameter. Experimental verification of this scaling hypothesis [3–5] was a key step in the development of a very sophisticated understanding of polymer solutions. Here, we use computer simulations to verify an analogous scaling hypothesis regarding the thermodynamics of block copolymers and to study universal characteristics of the order-disorder transition (ODT).

We consider a dense liquid of AB diblock copolymers, with N monomers per chain, and a fraction f_A of A monomers. We focus on the symmetric case $f_A = 1/2$. Self-consistent field theory (SCFT) is the dominant theoretical approach for block copolymers [6–8]. SCFT describes polymers as random walks with a monomer statistical segment length b, which we take to be equal for A and B monomers. The free energy cost of contact between A and B monomers is characterized by an effective Flory-Huggins interaction parameter χ_e. Let g denote a dimensionless excess free energy per chain, normalized by the thermal energy k_BT. SCFT predicts a free energy g for each phase that depends only upon f_A and the product $\chi_e N$, or upon $\chi_e N$ alone for $f_A = 1/2$. This yields a predicted phase diagram [6,7] that likewise depends only on f_A and $\chi_e N$. For $f_A = 1/2$, SCFT predicts a transition between the disordered and lamellar phases at $(\chi_e N)_{\mathrm{ODT}} = 10.495$.

SCFT has long been believed to be exact in the limit of infinitely long, strongly interpenetrating polymers [9,10]. The degree of interpenetration in a polymer liquid may be characterized by a dimensionless concentration $\bar{C} \equiv cR^3/N$, in which c is monomer concentration, c/N is molecule concentration, and $R = \sqrt{N}b$ is coil size. Alternatively, we may use the invariant degree of polymerization $\bar{N} \equiv \bar{C}^2 = N(cb^3)^2$ [10]. A series of post-SCFTs [10–18], starting with the Fredrickson-Helfand (FH) theory [10], has given predictions for *finite* diblock copolymers that depend on $\bar{N}$ in addition to the SCFT state parameters but that reduce to SCFT predictions in the limit $\bar{N} \to \infty$. Specifically, these theories suggest that, for symmetric copolymers, g is given in each phase by a universal (model- and chemistry-independent) function of $\chi_e N$ and $\bar{N}$ alone:

$$g = g(\chi_e N, \bar{N}). \tag{1}$$

If so, the value of $\chi_e N$ at the ODT (where the free energies of competing phases are equal) should depend only on $\bar{N}$ and should approach 10.495 as $\bar{N} \to \infty$. Equation (1) is a conjecture that is suggested by the mathematical structure of the FH theory. We show here, however, that this scaling hypothesis has a much wider range of validity than the theory that inspired it.

We compare simulations of four continuum bead-spring models (models H, $S1$, $S2$, and $S3$) and one lattice model (model F). Each bead-spring model has a harmonic bond potential and a nonbonded pair potential of the form $V_{ij}(r) = \epsilon_{ij}u(r)$, with $\epsilon_{AA} = \epsilon_{BB}$ and $\epsilon_{AB} \geq \epsilon_{AA}$. Model H uses a truncated purely repulsive Lennard-Jones pair potential (H denotes "hard") and is similar to the model of Grest and co-workers [19,20]. Models $S1$, $S2$, and $S3$ all use the softer pair potential typical of dissipative particle dynamics simulations. Model F is an fcc lattice model with 20% vacancies, an interaction ϵ_{AB} between unlike nearest-neighbor monomers, and no interaction between like monomers ($\epsilon_{AA} = \epsilon_{BB} = 0$). Models H [21–23], $S1$ [22,23], and F [24–27] have been studied previously. All bead-spring simulations reported here use accelerated NPT molecular dynamics [28] on Graphics Processing Units (GPUs). ODTs for bead-spring models were identified using a well-tempered metadynamics free energy method, as discussed in our Supplemental Material [29].

The word "model" is used here to refer to a set of choices for the functional form of the pair and bond potentials and for almost all parameters, except N and one parameter that is varied to control χ_e. Here, we vary the difference $\alpha \equiv \epsilon_{AB} - \epsilon_{AA}$, while holding T, pressure or monomer concentration, ϵ_{AA}, and all other parameters constant for each model.

The parameters of the four bead-spring models were chosen to facilitate testing of universality [Eq. (1)] by creating pairs of simulations of different models with unequal values of N but equal values of $\bar{N}$. Parameters for models H, $S1$, $S2$, and $S3$ were adjusted to give values of $\bar{N}/N = (cb^3)^2$ with ratios of nearly 1:4:16:32. Because simulations were conducted for chain lengths $N = 16$, 32, 64, and 128 that also differ by multiples of 2, some pairs of simulations of different models have equal values of $\bar{N}$. Specifically, systems H-64 (model H with $N = 64$) and $S1$-16 (model $S1$ with $N = 16$) both have $\bar{N} \simeq 240$, while $S1$-64 and $S2$-16 both have $\bar{N} \simeq 960$, systems $S1$-128, $S2$-32, and $S3$-16 all have $\bar{N} \simeq 1920$, and $S3$-64 and $S2$-32 both have $\bar{N} \simeq 3840$.

The simulations presented here span $\bar{N} \simeq 100$–7600, thus overlapping most of the range $\bar{N} \simeq 200$–20000 explored in experiments. For example, $\bar{N} \simeq 1100$ in a classic study of symmetric poly(styrene-*b*-isoprene) [38,39], $\bar{N} \simeq 220$ in a recent study of poly(isoprene- *b*-*L* lactic acid) [40], and $\bar{N} \simeq 5000$ in the study of poly (ethylene-propylene-*b*-ethyl ethylene) used to test the FH theory [41–44].

Estimating χ_e.—To compare results of different simulation models or experimental systems to coarse-grained theories, or to each other, one must somehow estimate how the interaction parameter χ_e for each model or chemistry depends on temperature T (in experiments) or simulation parameters. In our simulations, χ_e is an unknown model-dependent function $\chi_e(\alpha)$ of the control parameter α.

In previous simulations, $\chi_e(\alpha)$ has almost always been assumed to be a linear function of α, of the form $\chi_e(\alpha) \simeq z\alpha/k_BT$. Methods of estimating the coefficient z have generally relied [45] on either (1) some form of random-mixing approximation, thus ignoring monomer-scale correlations, or (2) a perturbation theory that allows a value for z to be obtained by analyzing intermolecular pair correlations in a reference homopolymer liquid [45–47]. The latter approach has been shown to give the first term of a Taylor expansion of $\chi_e(\alpha)$ in powers of α [47]. In recent studies of the structure factor $S(q)$ in the disordered phase [21,22], this perturbative estimate for χ_e was found to work well for small values of α (as expected) but to fail for the larger values of α reached near the ODT in most of the simulations considered here.

In the analysis of experimental data, the dependence of $\chi_e(T)$ upon temperature T is often estimated by fitting the structure factor $S(q, T)$ in the disordered phase to predictions of the RPA or FH theories. Below, we apply a similar analysis to simulation data for $S(q, \alpha)$. This approach is motivated by recent improvements in the agreement between theoretical predictions and simulation results for $S(q)$ in the disordered phase [23], which were obtained by using an improved theory for $S(q)$, the renormalized one-loop theory (ROL) [16,17], and (equally importantly) allowing χ_e to be a nonlinear function of α. In what follows, results for the free energy and ODT are thus analyzed and plotted using a nonlinear approximation for $\chi_e(\alpha)$ for each model that is obtained, as in Ref. [23], by doing a simultaneous fit of results for $S(q, \alpha)$ from simulations of several chain lengths to the ROL theory, while constraining the value of $d\chi_e(\alpha)/d\alpha$ at $\alpha = 0$ to agree with perturbation theory [29]. The need to allow for a nonlinear dependence of $\chi_e(\alpha)$ upon α implies that changes in α are inducing nonuniversal changes in monomer-scale correlations, in addition to universal changes in long-wavelength correlations.

Results.—We test Eq. (1) by comparing results from different simulation models and chain lengths for the molecular free energy g and its derivative $g' \equiv \partial g/\partial(\chi_e N)$. Given an adequate independent estimate of $\chi_e(\alpha)$, g' can be calculated from simulation data using the relation

$$\frac{\partial g}{\partial(\chi_e N)} = \frac{\langle U_{AB}(\alpha)\rangle}{MN\epsilon_{AB}(\alpha)} \left[k_B T \frac{d\chi_e(\alpha)}{d\alpha}\right]^{-1}, \qquad (2)$$

where U_{AB} is the total nonbonded AB pair interaction energy in a system of M chains. Equation (2) is derived by using the identity $\partial g/\partial\alpha = \langle\partial H(\alpha)/\partial\alpha\rangle/(k_BTM)$, where $H(\alpha)$ is the model Hamiltonian, to show that $\partial g/\partial\alpha = \langle U_{AB}\rangle/(Mk_BT\epsilon_{AB})$, and then writing $\partial g/\partial\chi_e = (\partial g/\partial\alpha)/(d\chi_e/d\alpha)$.

Equation (1) implies that $g' = \partial g/\partial(\chi_e N)$ should (like g) be a universal function of $\chi_e N$ and $\bar{N}$. Data from simulations of different models with matched values of $\bar{N}$ should thus collapse when g' is plotted vs $\chi_e N$. The quality of the collapse does, however, depend on the accuracy of the approximation for $\chi_e(\alpha)$ used to construct such a plot. The inset and main plots of Fig. 1 show two different attempts to collapse data for g' vs $\chi_e N$ for models $S1$-64 and $S2$-16, for which $\bar{N} \simeq 960$. The inset was constructed using the linear approximation [47] $\chi_e \simeq z\alpha/k_BT$. This approach fails, yielding a poor data collapse and poor agreement for the value $(\chi_e N)_{\mathrm{ODT}}$ of $\chi_e N$ at the ODT (arrows). The main plot was constructed using the nonlinear approximation for $\chi_e(\alpha)$ obtained by fitting $S(q)$. This succeeds, giving a nearly perfect collapse of data for g' and consistent values for $(\chi_e N)_{\mathrm{ODT}}$. Results for other pairs of models with matching $\bar{N}$ show similar agreement. The results verify both the scaling hypothesis [Eq. (1)] and the accuracy of this method of estimating $\chi_e(\alpha)$.

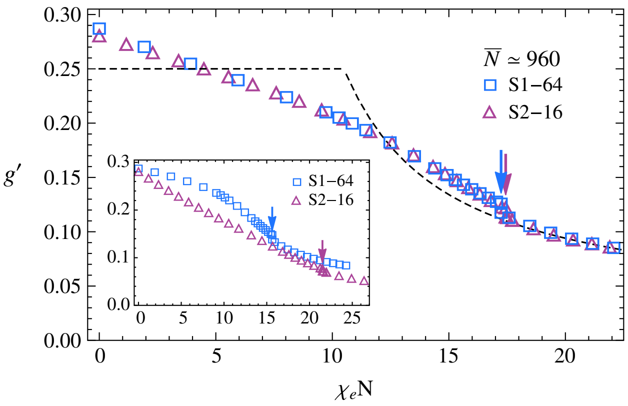

FIG. 1 (color online). Plot of $g' \equiv \partial g/\partial(\chi_e N)$ vs $\chi_e N$ for models S1-64 and S2-16 with matched $\bar{N} \simeq 960$. The dashed curve shows the SCFT prediction for $g'(\chi_e N)$. Vertical arrows mark the positions of the ODTs. Inset: Analogous plot using the simple linear approximation $\chi_e(\alpha) \simeq z\alpha/k_B T$.

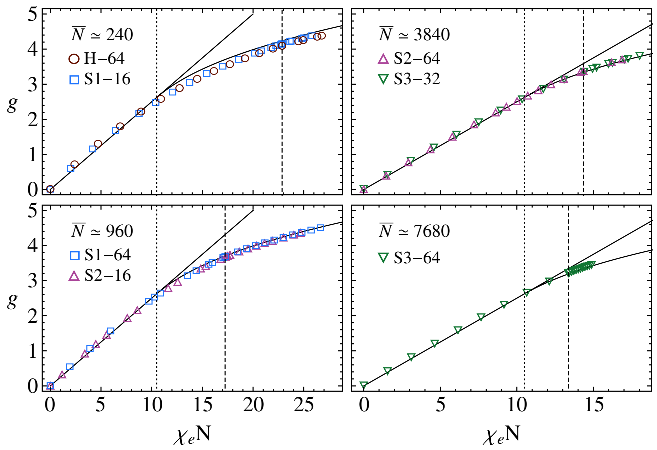

FIG. 2 (color online). Free energy per chain g vs $\chi_e N$ at four different values of $\bar{N}$, plotted using a nonlinear approximation for $\chi_e(\alpha)$. Solid lines are SCFT predictions for $g(\chi_e N)$. The straight solid line is the SCFT prediction $g(\chi_e N) = \chi_e N/4$ for a homogeneous phase. Vertical dotted lines show the SCFT ODT at $\chi_e N = 10.495$. Vertical dashed lines show actual ODTs. Where data are shown for two systems, the ODT is shown for the system with larger N.

There is a small but measurable discontinuity $\Delta g'$ in g' across the ODT in Fig. 1, as expected for a first-order transition. The smallness of the discontinuity ($\Delta g' \simeq 0.008$, or 7%) indicates that the degree of AB contact is similar in the disordered and ordered phases near the ODT. This suggests that the disordered phase has a local structure rather similar to that of the ordered phase, with well-defined A and B domains and a similar AB interfacial area per volume, but without long-range order. The SCFT prediction for $g'(\chi_e N)$ (dashed line) is given by the spatial average of the product $\phi_A(\mathbf{r})\phi_B(\mathbf{r})$ of the predicted local volume fractions of A and B monomers. This yields $g' = 0.25$ in the disordered phase, at $\chi_e N < 10.495$. Interestingly, SCFT predictions for g' are poor in the disordered phase near the ODT but show excellent agreement with simulations in the ordered phase. SCFT thus accurately predicts the extent of AB contact within the ordered phase but is intrinsically incapable of handling the strong short-range correlations in the disordered phase.

Figure 2 shows the free energy per chain g vs $\chi_e N$ for four values of $\bar{N}$. These were calculated by numerically integrating simulation results for $\partial g/\partial\alpha$ within each phase, setting $g = 0$ at $\alpha = 0$ by convention, and equating values of g in the two phases at the observed ODT. Three of the plots show overlapping results for pairs of simulations with matched values of $\bar{N}$, again demonstrating universality. In the range $10.495 < \chi_e N < (\chi_e N)_{\rm ODT}$ in which the disordered phase develops strong correlations, simulation results fall well below the SCFT prediction for a homogeneous phase (the straight line) and actually lie much closer to SCFT predictions for the *ordered* phase. Interestingly, SCFT predictions for g are rather accurate within the ordered phase for all but the lowest value of $\bar{N}$ shown here and seem to become more so with increasing $\bar{N}$. This agreement does not follow trivially from the observed accuracy of SCFT predictions for g' in the ordered phase, since the value of g at the ODT has been calculated by integrating $\partial g/\partial\alpha$ through the disordered phase, in which SCFT predictions for g' are poor. Physically, the main components of g are free energies arising from AB contact and chain stretching. Only the extent of AB contact is directly reflected by the value of g'. Our results thus imply that SCFT accurately describes both main components of g in the ordered phase, although not in the disordered phase near the ODT.

The main plot of Fig. 3 shows a compilation of results for $(\chi_e N)_{\rm ODT}$ from all simulations plotted vs $\bar{N}$, using our nonlinear fits for $\chi_e(\alpha)$. The inset shows a corresponding

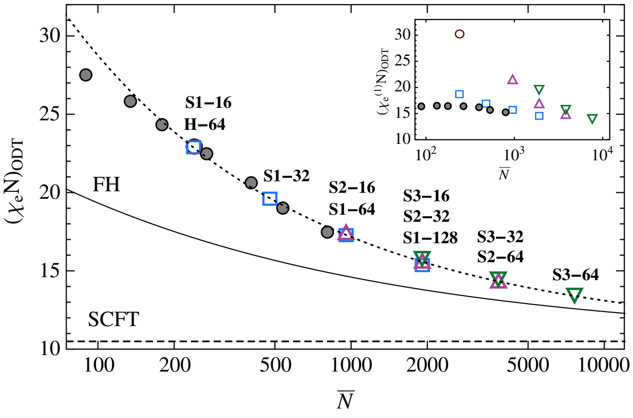

FIG. 3 (color online). Values of $\chi_e N$ at the ODT vs $\bar{N}$, for all simulations. Bead-spring model results are shown as open symbols, with labels for specific systems. Lattice model results for $N = 20$, 30, 40, 60, 90, 120, and 180 are filled gray circles. The short-dashed curve is the empirical fit in Eq. (3), the solid curve is the FH prediction, and the horizontal long-dashed line is the SCFT prediction. Inset: Analogous plot using the linear approximation $\chi_e^{(1)}(\alpha) \equiv z\alpha/k_B T$ to plot the ODT vs $\bar{N}$.

plot constructed using the perturbative linear approximation for $\chi_e(\alpha)$. As before (inset of Fig. 1), the linear approximation fails to collapse the data. With the nonlinear $\chi_e(\alpha)$, however, the results from all five models collapse onto a master curve, as required by Eq. (1). Note particularly the nearly perfect agreement between simulations with matched values of $\bar{N}$, illustrated by overlapping open symbols. The dotted curve is an empirical fit

$$(\chi_e N)_{\mathrm{ODT}} = 10.495 + 41.0\bar{N}^{-1/3} + 123.0\bar{N}^{-0.56} \tag{3}$$

to the bead-spring model results, in which the first two terms give the FH prediction [10] (solid curve). These results suggest that the FH theory becomes accurate for $\bar{N} \gtrsim 10^4$ but breaks down at the lower values of $\bar{N} \lesssim 10^4$ typical of experiments.

Insight into why the FH theory fails for $\bar{N} \lesssim 10^4$ can be gained by examining composition profiles near the ODT. The FH theory assumes weak segregation at the ODT. The inset of Fig. 4 shows the dependence of the average local volume fraction $\phi_A(z)$ of A monomers in the lamellar phase at the ODT, for model $S1$-64 ($\bar{N} \simeq 960$). This quantity exhibits a rather large amplitude oscillation, yielding a maximum $\max[\phi_A(z)] \simeq 90\%$ in the middle of the A domain. The function $\phi_A(z)$ is also almost perfectly sinusoidal (ratio of the third to the first harmonic: 1.6%), but we believe that this is partly a result of smearing by interfacial fluctuations. The main plot shows how the value of $\max[\phi_A(z)]$ at the ODT varies with $\bar{N}$. This value is large over the entire range studied here but decreases slowly with $\bar{N}$ in a manner consistent with convergence to the FH prediction (solid curve) for $\bar{N} \gtrsim 10^4$. Note that the FH theory predicts unphysical values of $\max[\phi_A(z)] > 1$ for $\bar{N} \lesssim 10^3$, implying that lower values are well beyond its region of validity.

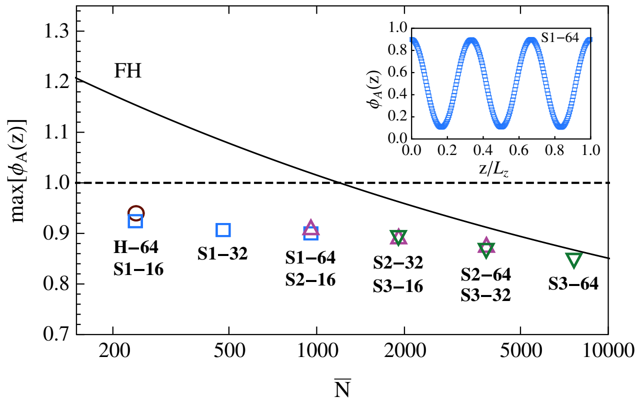

FIG. 4 (color online). Maximum of the average volume fraction $\phi_A(z)$ of A monomers in the ordered phase at the ODT plotted vs $\bar{N}$ for all bead-spring simulations. The solid curve is the FH prediction. The horizontal dashed line is the bound $\phi_A(z) = 1$, above which the prediction becomes unphysical. Inset: $\phi_A(z)$ for model $S1$-64, where the coordinate z is normal to the layers and L_z is the size of the simulation cell.

In this work, we provide the first compelling evidence for a universal dependence of thermodynamic properties of block copolymer melts on $\bar{N}$, by collapsing results obtained with different simulation models. The scaling hypothesis of Eq. (1) is found to hold even for surprisingly short chains, down to at least $\bar{N} \sim 200$. We also provide the first reliable estimate of how the value of $(\chi_e N)_{\mathrm{ODT}}$ actually depends on $\bar{N}$, given by Eq. (3). The FH theory appears to be quantitatively accurate for $\bar{N} \gtrsim 10^4$ but fails at lower values typical of most experiments, for which the ordered and disordered phases both become rather strongly segregated near the ODT. SCFT gives poor predictions for $(\chi_e N)_{\mathrm{ODT}}$ but gives surprisingly accurate predictions for the free energy of the ordered lamellar phase, suggesting that SCFT may provide more reliable predictions for order-order transitions.

Our success in collapsing data from different simulation models relied critically upon the adoption of a more sophisticated method of estimating χ_e than used in previous studies of the ODT. Here, χ_e is determined by fitting disordered state data for $S(q)$ from each model to the ROL theory, while allowing for a nonlinear dependence of χ_e upon α. The absence of an adequate method of estimating χ_e has, until now, made it impossible to perform precise comparisons of coarse-grained simulation of block copolymers to theoretical predictions, other simulation models, or experiments. Our procedure for estimating χ_e can also be applied to experiments, by fitting measured scattering intensities to the ROL theory to estimate $\chi_e(T)$. Alternatively, χ_e could be deduced by fitting the experimental ODTs to our improved estimate of $(\chi_e N)_{\mathrm{ODT}}$. Interaction parameters obtained by analyzing simulations and experiments involving symmetric block copolymers can be used to predict the behavior of more complicated systems, such as multiblock copolymer melts. The demonstration of universality, combined with an accurate, broadly applicable method of determining χ_e, promises a major improvement in the ability of coarse-grained simulations to make reliable quantitative predictions about real materials.

We acknowledge fruitful discussions with Juan de Pablo and Jian Qin and thank Michael Engel for carefully reading the manuscript. This work was supported by NSF Grants No. DMR-0907338 and No. DMR-1310436, the EPSRC (EP/E10342/1), a DFG postdoctoral fellowship (GL 733/1-1) (J. G.), and a University of Minnesota doctoral fellowship (P. M.). The research used resources of the Minnesota Supercomputing Institute and of the Keeneland Computing Facility, which is supported by NSF Contract No. OCI-0910735.

---

[*] Corresponding author.
morse012@umn.edu

[†] Present address: Department of Chemical Engineering, University of Michigan, Ann Arbor, MI 48109, USA.

[‡] Present address: Institute for Nanotechnology, University of Waterloo, QNC 5602, Waterloo, Ontario N2L 3G1, Canada.

[1] P.-G. de Gennes, *Scaling Concepts in Polymer Physics* (Cornell University Press, Ithaca, NY, 1979).
[2] L. Schaefer, *Excluded Volume Effects in Polymer Solutions* (Springer-Verlag, Berlin, 1999).
[3] W. Graessley, *Polymeric Liquids and Networks: Structure and Properties* (Taylor & Francis, New York, 2004).
[4] M. Daoud, J. Cotton, B. Farnoux, G. J. G. Sarma, C. D. H. Benoit, C. Picot, and P. de Gennes, Macromolecules **8**, 804 (1975).
[5] I. Noda, N. Kato, T. Kitano, and M. Nagasawa, Macromolecules **14**, 668 (1981).
[6] L. Leibler, Macromolecules **13**, 1602 (1980).
[7] M. W. Matsen and M. Schick, Phys. Rev. Lett. **72**, 2660 (1994).
[8] M. W. Matsen, J. Phys. Condens. Matter **14**, R21 (2002).
[9] P. G. de Gennes, J. Phys. Lett. **38**, 441 (1977).
[10] G. H. Fredrickson and E. Helfand, J. Chem. Phys. **87**, 697 (1987).
[11] J.-L. Barrat and G. H. Fredrickson, J. Chem. Phys. **95**, 1281 (1991).
[12] M. Olvera de la Cruz, Phys. Rev. Lett. **67**, 85 (1991).
[13] A. M. Mayes and M. Olvera de la Cruz, J. Chem. Phys. **95**, 4670 (1991).
[14] R. Holyst and A. Vilgis, J. Chem. Phys. **99**, 4835 (1993).
[15] P. Beckrich, A. Johner, A. N. Semenov, S. P. Obukhov, H. Benoît, and J. P. Wittmer, Macromolecules **40**, 3805 (2007).
[16] P. Grzywacz, J. Qin, and D. C. Morse, Phys. Rev. E **76**, 061802 (2007).
[17] J. Qin, P. Grzywacz, and D. C. Morse, J. Chem. Phys. **135**, 084902 (2011).
[18] D. C. Morse and J. Qin, J. Chem. Phys. **134**, 084902 (2011).
[19] G. S. Grest, M.-D. Lacasse, K. Kremer, and A. M. Gupta, J. Chem. Phys. **105**, 10583 (1996).
[20] M. Murat, G. S. Grest, and K. Kremer, Macromolecules **32**, 595 (1999).
[21] J. Qin and D. C. Morse, Phys. Rev. Lett. **108**, 238301 (2012).
[22] J. Glaser, J. Qin, P. Medapuram, M. Mueller, and D. Morse, Soft Matter **8**, 11310 (2012).
[23] J. Glaser, J. Qin, P. Medapuram, and D. Morse, Macromolecules **47**, 851 (2014).
[24] O. N. Vassiliev and M. W. Matsen, J. Chem. Phys. **118**, 7700 (2003).
[25] M. W. Matsen, G. H. Griffiths, R. A. Wickham, and O. N. Vassiliev, J. Chem. Phys. **124**, 024904 (2006).
[26] T. Beardsley and M. Matsen, Eur. Phys. J. E **32**, 255 (2010).
[27] T. Beardsley and M. Matsen, Macromolecules **44**, 6209 (2011).
[28] J. A. Anderson, C. D. Lorenz, and A. Travesset, J. Comput. Phys. **227**, 5342 (2008).
[29] See Supplemental Material at http://link.aps.org/supplemental/10.1103/PhysRevLett.113.068302, for detailed models and methods, which includes Refs. [30–37].
[30] G. J. Martyna, D. J. Tobias, and M. L. Klein, J. Chem. Phys. **101**, 4177 (1994).
[31] J. Qin and D. C. Morse, J. Chem. Phys. **130**, 224902 (2009).
[32] A. Laio and M. Parrinello, Proc. Natl. Acad. Sci. U.S.A. **99**, 12 562 (2002).
[33] A. Barducci, G. Bussi, and M. Parrinello, Phys. Rev. Lett. **100**, 020603 (2008).
[34] R. W. Hockney and J. W. Eastwood, *Computer Simulation Using Particles* (Taylor and Francis, New York, 1988).
[35] http://github.com/jglaser/metadynamics-plugin.
[36] R. H. Bisseling, *Parallel Scientific Computation* (Oxford University Press, New York, 2004).
[37] http://github.com/jglaser/dfftlib.
[38] F. S. Bates, M. F. Schulz, A. K. Khandpur, S. Förster, J. H. Rosedale, K. Almdal, and K. Mortensen, Faraday Discuss. **98**, 7 (1994).
[39] A. Khandpur, S. Foerster, F. Bates, I. Hamley, A. Ryan, W. Bras, K. Almdal, and K. Mortensen, Macromolecules **28**, 8796 (1995).
[40] S. Lee, T. Gillard, and F. Bates, AIChE J. **59**, 3502 (2013).
[41] F. S. Bates, J. H. Rosedale, G. H. Fredrickson, and C. J. Glinka, Phys. Rev. Lett. **61**, 2229 (1988).
[42] F. S. Bates, J. H. Rosedale, and G. H. Fredrickson, J. Chem. Phys. **92**, 6255 (1990).
[43] J. H. Rosedale, F. S. Bates, K. Almdal, K. Mortensen, and G. D. Wignall, Macromolecules **28**, 1429 (1995).
[44] J. Qin, Ph. D. thesis, University of Minnesota, 2009.
[45] M. Müller, *Comparison of Self-Consistent Field Theory and Monte Carlo Simulations*, in Soft Matter, Volume 1: Polymer Melts and Mixtures, edited by G. Gompper and M. Schick, (Wiley-VCH Verlag GmbH & Co. KGaA, Weinheim, Germany, 2007).
[46] M. Mueller and K. Binder, Macromolecules **28**, 1825 (1995).
[47] D. C. Morse and J. Chung, J. Chem. Phys. **130**, 224901 (2009).